Solar Physics (2005) 231: 45–70

CORONAL FLUX RECYCLING TIMES

R. M. CLOSE and C. E. PARNELL
School of Mathematics and Statistics, University of St. Andrews, St. Andrews, Fife, KY16 9SS Scotland, U.K.
(e-mail: robertc@mcs.st-and.ac.uk)

D. W. LONGCOPE
Department of Physics, Montana State University, Bozeman, MT 59717, U.S.A.

and

E. R. PRIEST
School of Mathematics and Statistics, University of St. Andrews, St. Andrews, Fife, KY16 9SS Scotland, U.K.

(Received 22 March 2005; accepted 22 April 2005)

Abstract. High-cadence, high-resolution magnetograms have shown that the quiet-Sun photosphere is very dynamic in nature. It is comprised of discrete magnetic fragments which are characterized by four key processes – emergence, coalescence, fragmentation and cancellation. All of this will have consequences for the magnetic field in the corona above.

The aim of this study is to gauge the effect of the behavior of the photospheric flux fragments on the quiet-Sun corona. By considering a sequence of observed magnetograms, photospheric flux fragments are represented by a series of point sources and the resulting potential field arising from them is examined. It is found that the quiet-Sun coronal flux is generally recycled on time scales considerably shorter than the corresponding time scales for the recycling of photospheric flux. From the motions of photospheric fragments alone, a recycling time of coronal flux of around 3 h is found. However, it is found that the amount of reconnection driven by the motions of fragments is comparable to the amount driven by emergence and cancellation of flux, resulting in a net flux replacement time for the corona of only 1.4 h.

The technique used in this study was briefly presented in a short research letter (R. M. Close *et al.*, *Astrophys. J.*, **612**, L81, 2004); here the technique is discussed in far greater depth. Furthermore, an estimate is made of the currents required to flow along separator field lines in order to sustain the observed heating rates (assuming separator reconnection is the key mechanism by which the solar corona is heated).

1. Introduction

Observations have shown that the outer atmosphere of the Sun, the corona, is heated to a temperature of several million Kelvin, some two orders of magnitude hotter than the chromosphere below. It is believed that the energy required for such heating originates in the turbulent convection zone below the photosphere. This energy is channeled through the solar surface into the chromosphere and corona by the magnetic field.

The presence of the magnetic field is the product of complex dynamo processes. In the case of active regions, this is most probably the direct consequence of a global magnetic field generation mechanism situated at the base of the convection zone, where differential rotation generates a toroidal field from poloidal field (Moffat, 1978). The origin of the quiet-Sun field, on the other hand, is not known with such certainty. One possibility is that it is a by-product of the same large-scale solar dynamo that gives rise to the active regions (Spruit, Title, and Ballegooijen, 1997). However, the continued presence of the quiet-Sun fields at solar minimum (when active regions are generally absent) has led to the suggestion that the quiet-Sun photospheric flux is generated by local dynamo action just below the Sun's surface driven by granular and supergranular flows (Meneguzzi and Pouquet, 1989; Durney, Young, and Roxburgh, 1993; Petrovay and Szakály, 1993; Lin, 1995; Hughes, Cattaneo, and Kim, 1998; Tobias, 2002). In practice, it is likely that both mechanisms are at work, so that the problem lies with determining how substantial a role each mechanism plays in the generation of the quiet-Sun magnetic fields.

In the photosphere, new flux is seen to be constantly emerging. Hagenaar (2001) measured the rate of this emergence and showed that enough flux is emerging for the entire quiet-Sun flux to be recycled in around only 14 h. (This figure was revised to 8–19 h by Hagenaar, Schrijver, and Title (2003)). The continual emergence of flux is matched by continued cancellation between merged and fragmented flux concentrations, so that the picture that emerges is one of a very dynamic quiet-Sun magnetic field. Schrijver *et al.* (1997) showed that observed flux distributions are not consistent with a source function that is just the distribution of flux that disappears from the solar surface. Hence, the magnetic fields are not simply bobbing up and down through the photosphere, and are instead being continually reprocessed. Supergranular flows sweep magnetic fields to supergranular cell boundaries, fragmenting, canceling or merging them along the way. Upon reaching a cell boundary, flux fragments then move along the boundary with the flow along it and are again subjected to fragmentation, cancellation or mergence.

The complicated motions of magnetic flux fragments in the quiet-Sun network will drive reconnection higher in the upper atmosphere, as magnetic fields constantly realign themselves in response to the ever-changing footpoint configurations. Moreover, new flux that emerges through the photospheric surface will at some stage reconnect with the overlying field.

Several models have been presented for the way in which energy is dissipated in the corona. In particular, reconnection of magnetic field lines in the corona may result in energy being deposited there (Priest and Forbes, 2000, and references therein). This process of magnetic reconnection is thought to occur in many quiet-Sun coronal events, including X-ray bright points, X-ray jets and nanoflares.

Reconnection driven by the magnetic carpet is important, since it is thought that this is the mechanism by which the ambient corona is heated (Levine, 1974; Parker, 1981, 1983, 1988; Parnell and Priest, 1994, 1995; Schrijver *et al.*, 1998; Longcope

and Kankelborg, 1999; Priest, Heyvaerts, and Title, 2002). It may also play a role in accelerating the fast solar wind (McKenzie, Banaszkiewicz, and Axford, 1995).

Thus, the aim of this study is to try to put a handle on the amount of reconnection that occurs as a consequence of the dynamic nature of the magnetic carpet. This is approached by taking observed magnetograms, identifying and tracking individual fragments, and extrapolating the magnetic field using a potential field approximation. By comparing domain fluxes between successive magnetogram images, the amount of reconnection that must have taken place to move from one configuration to the next is gauged. Section 2 discusses how photospheric flux fragments are treated using the general approach of Longcope (2001) for mapping the connectivity of the field, whilst Section 3 details various assumptions in the analysis. This is followed up with an analysis whereby emergence and cancellation are prohibited in Section 4. Section 5 starts with a discussion regarding changes in source fluxes, which is followed by calculations of flux recycling times due to emergence and cancellation. An estimate of the amount of reconnection that takes place when emergence and submergence are allowed is then presented. The study is rounded off with a discussion of energy dissipation due to separator reconnection in Section 6. A concluding discussion is given in Section 7.

2. Photospheric Flux Fragments

To study the effects of granular and supergranular flows on the connectivity of magnetic carpet fields, a sequence of high-resolution MDI magnetograms (each 240 Mm $\times$ 240 Mm) is used for the analysis, and the central 80 Mm $\times$ 80 Mm is studied. After averaging over sequences of 15-magnetograms spaced by 1 min (in order to reduce the effects of 5 min oscillations), this leaves a series of 50 magnetograms, each spaced by 15 min and covering a 12-h period.

Discrete fragments are located spatially and labeled in each of the 50 magnetograms in turn. On average, there are 286 fragments in total per frame, although naturally this number varies from frame to frame. Subsequent magnetograms are then compared in order to track the motions of individual fragments. Thus, the unique labels given to each fragment are projected temporally through the set of magnetograms (Parnell, in preparation).

In the model considered here, the photosphere is treated locally as the plane $z = 0$, and the corona is the region $z > 0$. Since magnetograms show that the photospheric magnetic field is generally assembled into isolated fragments of strong magnetic field (a small section of which is illustrated in Figure 1 (*left*)), with relatively little field outwith these concentrations, each fragment is represented by a single point source, placed at its centroid. As only the region $z \geq 0$ is considered here, the sources are treated as points where flux passes through the $z = 0$ plane and are thus not isolated monopoles (which are not allowed since $\nabla \cdot \mathbf{B} = 0$). The potential field is obtained using the point-source Poisson solution, which gives the

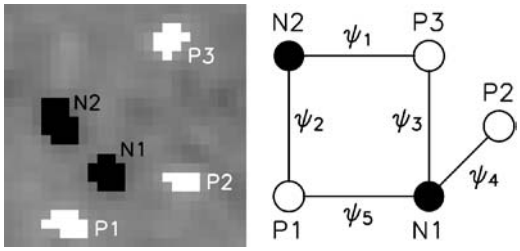

Figure 1. (*Left*) A small section of one of the Magnetogram images showing a typical quiet-Sun region containing mixed-polarity fragments. The field shown here consists of three positive fragments, P_1, P_2 and P_3, and two negative fragments, N_1 and N_2. The background shown in grey is, by comparison with the flux fragments, unmagnetized. (*Right*) A possible domain graph for the region, with the domain fluxes ψ_i ($i = 1 \ldots 5$) indicated.

magnetic field $\mathbf{B}(\mathbf{r})$ at a point $\mathbf{r} = x\hat{\mathbf{x}} + y\hat{\mathbf{y}} + z\hat{\mathbf{z}}$ by the following sum over all the sources

$$\mathbf{B}(\mathbf{r}) = \sum_i \frac{\epsilon_i \, (\mathbf{r} - \mathbf{r_i})}{|\mathbf{r} - \mathbf{r_i}|^3} \, , \tag{1}$$

where $\mathbf{r_i} = x_i\hat{\mathbf{x}} + y_i\hat{\mathbf{y}} + z_i\hat{\mathbf{z}}$ is the position of the ith source, with strength ϵ_i.

As there are no magnetic monopoles within the Sun, the net flux crossing the complete solar surface must be zero. However, in a case such as the one studied here, where only a particular section of the photospheric surface is studied, there will undoubtedly be, unless one is extremely lucky, some amount of flux imbalance. Thus, if a flux imbalance in a particular region is found, and the sum of all the source fluxes is

$$\sum_a \Phi_a = \Phi_{\mathrm{Tot}}, \tag{2}$$

then this requires the inclusion, at infinity, of a source with flux $-\Phi_{\mathrm{Tot}}$. Thence, each system may be considered to be in flux balance.

Aside from topologically defining field lines, such as fan field lines, spine field lines and separator field lines, every field line in the corona begins at a positive source and ends at a negative source. In this scenario, the coronal volume may be viewed as being comprised of a multitude of flux domains, each characterized by the end-points of its field lines.

It is, of course, possible that a pair of sources may be connected by field lines from multiple domains. However, in this study, only changes in the total flux connecting pairs of sources will be considered, and any reconnection that relates to reapportionment of flux between any multiple domains connecting the given pair of sources will be neglected, just as any redistribution of field lines within domains will not be accounted for.

The fluxes of the $N_{\rm d}$ domains that interconnect the $N_{\rm s}$ sources will be denoted by ψ_n. If a source a is considered, with a flux Φ_a, then the $N_{\rm d}$ domain fluxes may be related to the flux of source a through the incidence matrix

$$\Phi_a = \sum_{n=1}^{N_{\rm d}} M_{an}\psi_n. \tag{3}$$

The domain fluxes ψ_n are defined as positive quantities. An *unsigned-flux convention* is adopted here, whereby $\Phi_a > 0$ for all sources, and the entries in M_{an} are either $+1$ or 0. Longcope and Klapper (2002), by contrast, use a *signed-flux convention*, where $\Phi_a < 0$ if a is a negative-polarity source, and along the corresponding row $M_{an} = -1$ for each domain n connected to it. The unsigned-flux convention is opted for here so as to avoid confusion with the terms "increase" and "decrease" when referring to changes in source fluxes. This will become important when comparing emergence and cancellation of flux in a given domain with reconnection in that domain.

Figure 1 (*right*) shows an example of how a magnetic field may be interpreted in terms of graph theory. In this example,

$$M = \begin{array}{c} \\ P1 \\ P2 \\ P3 \\ N1 \\ N2 \end{array} \begin{array}{c} \begin{array}{ccccc} \mathcal{D}_1 & \mathcal{D}_2 & \mathcal{D}_3 & \mathcal{D}_4 & \mathcal{D}_5 \end{array} \\ \begin{pmatrix} 0 & 1 & 0 & 0 & 1 \\ 0 & 0 & 0 & 1 & 0 \\ 1 & 0 & 1 & 0 & 0 \\ 0 & 0 & 1 & 1 & 1 \\ 1 & 1 & 0 & 0 & 0 \end{pmatrix} \end{array}, \tag{4}$$

where $\mathcal{D}_i$ denotes the domain within which the flux ψ_i is contained. The relationship (3) may be stated more explicitly as

$$\begin{pmatrix} \Phi_1 \\ \Phi_2 \\ \Phi_3 \\ \Phi_4 \\ \Phi_5 \end{pmatrix} = \begin{pmatrix} 0 & 1 & 0 & 0 & 1 \\ 0 & 0 & 0 & 1 & 0 \\ 1 & 0 & 1 & 0 & 0 \\ 0 & 0 & 1 & 1 & 1 \\ 1 & 1 & 0 & 0 & 0 \end{pmatrix} \cdot \begin{pmatrix} \psi_1 \\ \psi_2 \\ \psi_3 \\ \psi_4 \\ \psi_5 \end{pmatrix}. \tag{5}$$

3. Analysis

The sequence of 50 magnetograms gives a total of 49 sets of consecutive pairs of magnetograms with which to compare domain fluxes. Henceforth, the first

magnetogram in a pair shall be denoted with the letter 'i' for initial, and the second magnetogram with the letter 'f' for final. In order to obtain the domain fluxes ψ_n, the same method as in Close *et al.* (2003) is used. This involves calculating a number of field lines from starting points close to each source. Hence, from each source within the inner region, m field lines are traced, with m equal to the integer part of ϵ/ϵ_1 (where $\epsilon_1 = 7.73 \times 10^{15}$ Mx). Thus, each field line represents essentially the same amount of flux.

The connectivity for each magnetogram is stored in a connectivity matrix, where columns represent positive-polarity fragments and rows represent negative fragments. Naturally, the nature of the connectivity matrix will change from one magnetogram to the next, as fragments may emerge, fragment, coalesce or disappear from one magnetogram to the next. Thus, positive and negative index vectors are kept for each frame, and the history of which fragments have fragmented and which have coalesced is also stored. This enables a comparison of domain fluxes for each of the 49 pairs. To accommodate for the fact that field lines may close outwith the inner region, all the flux represented by such field lines is recorded in the connectivity matrix; however, only half the flux represented by a field line closing within the inner region is recorded because, at least in optimal conditions, the other half of the flux represented will be recorded when tracing back from the fragment at which the field line closed. Thus, all the flux within the inner region studied is accounted for.

3.1. Comparing magnetogram pairs

Taking each pair of magnetograms in turn, the aim is to have, for every fragment in frame f, a corresponding fragment in frame i, and vice versa. However, a complication arises due to the fact that fragments may split or coalesce. The exact cause of fragmentation is not clear, but it is suspected that granulation may play a role (Parnell, 2001). A given network element may cover a region containing as many as 25 granules, so it is quite probable that granulation flows will constantly buffet the many intense flux tubes comprising the magnetic fragments, resulting in a continuous redistribution of the flux within each fragment. Supergranular flows will tend to hold these fragments together as they drift towards the downflow regions at supergranular boundaries. However, whenever there is a weakening in the supergranular flows, then granular motions will prevail, causing fragmentation to occur.

Sketched in Figure 2 are three possible scenarios that may occur involving fragmentation and coalescence. Figure 2(a) shows a fragment in frame i that has split into several smaller fragments by frame f. Figure 2(b) shows the converse of this, where several distinct fragments in frame i have merged into a single, larger fragment by frame f. However, a third possibility, shown in Figure 2(c), is that several fragments in frame i coalesce into a single, larger fragment, which itself is viewed to have split by frame f. Note the suggestion here is that coalescence occurred, followed by fragmentation. Of course, one cannot know what happened

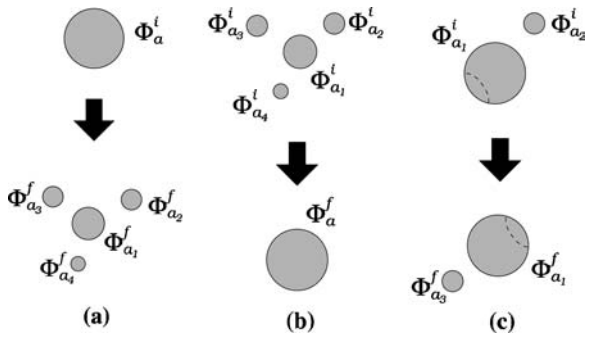

Figure 2. Sketches of the possible scenarios that may arise when (a) a single fragment in frame i has split into several smaller fragments by frame f, (b) several fragments in frame i have merged into a single, larger fragment by frame f, and (c) several fragments merge to form a single larger fragment in frame i, whilst this single fragment has split into several smaller fragments by frame f. The various Φ values represent the flux in the given fragments.

between frames, so it is equally plausible that fragmentation occurred, followed by coalesence. Indeed, both processes may have occurred at the same time. However, the way such cases are treated is independent of the order of the processes.

Fragmentation and coalescence may be dealt with in the following way. Consider two fragments, a and b, in frame f, with fluxes Φ_a^f and Φ_b^f, respectively. If these two fragments are connected by an amount ψ_n^f, then the change in the flux connecting a and b from frame i to frame f may be written as

$$\Delta\psi_n = \psi_n^f - \kappa_A \kappa_B \psi_N^i. \tag{6}$$

The term $\kappa_A \kappa_B \psi_N^i$ is essentially ψ_n^i, the amount of flux connecting the equivalents of the fragments a and b in the frame i. The values of κ_A and κ_B, which deal with fragmentation, and ψ_N^i, which deals with mergence, are found in the following manner. If fragment a in frame f has been formed by fragmentation, then

$$\kappa_A = \frac{\Phi_a^f}{\Phi_A^f}, \tag{7}$$

where Φ_A^f is the sum of the fluxes of all the fragments that were involved in the fragmentation. Otherwise $\kappa_A = 1$. κ_B is defined in a similar way for the fragment b. Thus, it is assumed that, at the point of fragmentation, each fragment receives a portion of the connected flux proportional to its own flux strength.

The value of ψ_N^i is defined in one of the following three ways.

1. If both the fragments a and b consist of fragments that merged between the frames i and f, then

$$\psi_N^i = \sum_{j,k} \text{Flux connecting } a_j^i \text{ to } b_k^i,$$

where the a^i_j are the fragments associated with a that have merged by frame f, and the b^i_j are the fragments associated with b that have merged by frame f.

2. If only a consists of fragments that merged between the frames i and f, then

$$\psi^i_N = \sum_j \text{Flux connecting } a^i_j \text{ to } b^i,$$

where the a^i_j are the fragments associated with a that have merged by frame f, and b^i is the fragment associated with b in the frame i.

3. If neither a nor b consist of fragments that merged between the frames i and f, then

$$\psi^i_N = \text{Flux connecting } a^i \text{ to } b^i,$$

where a^i is the fragment associated with a in the frame i, and b^i is the fragment associated with b in the frame i.

Births and deaths of fragments cause a slight problem, as it is of course not possible to find corresponding fragments in both frames when fragments simply appear/disappear between frames. The way in which this problem is overcome is as follows. If a fragment in magnetogram i has died by magnetogram f, then either (i) the fragment is removed from frame i or (ii) the fragment is copied into frame f, giving it the same flux and the same position as it has in frame i. Both of these options are deployed in different scenarios later on. Fragments that are newly born in frame f are treated in an analogous manner.

3.2. Emergence, cancellation and reconnection

In complex magnetic configurations, such as those found in the mixed-polarity quiet Sun, the motions of photospheric fragments will inevitably, at the very least, lead to a redistribution of flux between the domains that have their flux rooted in these fragments. Also, from a topological viewpoint, these motions will drive bifurcations, as old domains are destroyed or altered and new ones are created (Brown and Priest, 1999, 2001; Beveridge, Priest, and Brown, 2002). In a potential field, the system is entirely current-free, so the configuration permits no stress and therefore changes in connectivity occur instantly. Here, however, the details of how the reconnection occurs are not considered; instead, snapshots of the field are examined as the process evolves, and regions where reconnection has occurred are identified.

The motions of the flux fragments are not the only reason for changes in domain fluxes, though. In a system as dynamic as the quiet-Sun photosphere, emergence and cancellation of flux through the photospheric boundary will also alter domain fluxes, so that the resulting changes that are recorded from one magnetogram to the next will be the net effect of emergence, cancellation and reconnection. In light

of this, recycling times for coronal flux in two different scenarios are considered here. In the first, reconnection is driven purely through the motions of the fragments by prohibiting emergence and cancellation. In this case, fluxes are averaged between frames, so that fragment strengths are kept fixed and only the effects of the motions of the fragments are measured. In the second scenario, emergence and cancellation are allowed, so that the fluxes of the fragments may vary between frames. Births and deaths of fragments are exceptions to this; by either (i) copying the newly born/just died fragments into the frame in which they are not present, or (ii) removing the newly born/just died fragments completely (both of these tricks were discussed in Section 3.1), it is essentially assumed that these fragments have witnessed no emergence or cancellation. Although this will introduce slight errors into the analysis, the alternative, whereby the fragments are copied into the frame in which they are absent but have their fluxes set to zero (these would essentially be "ghost fragments", existing solely for the purpose of quantifying the change in domain fluxes), would introduce far greater errors into the analysis. This is mainly because the cadence of the magnetogram images is not high enough to trace the deaths (births) smoothly, resulting in a vanishing effect whereby fragments suddenly disappear (appear), rather than having their strengths decrease (increase) to (from) zero. This shall be discussed further later on.

From a coronal heating viewpoint, a measure of the amount of reconnection that occurs is what is of greatest interest. Changes in source fluxes are accompanied by changes in domain fluxes, related by the expression

$$\Delta\Phi_a = \sum_{n=1}^{N_\mathrm{d}} M_{an}\,\Delta\psi_n. \tag{8}$$

This assumes that the connectivity does not change, so that, if a domain is absent from either the initial or final field, then it is simply included in the incidence matrix and given the value $\psi_n = 0$. Magnetic reconnection is a change in domain fluxes, $\Delta\psi_n = R_n$, which occurs in the corona and therefore does not affect the source fluxes. Thus

$$\sum_{n=1}^{N_\mathrm{d}} M_{an} R_n = 0. \tag{9}$$

The processes of emergence and cancellation of flux will alter the fluxes of the photospheric sources, which in turn will inject flux S_n into the domains. In general, domain fluxes combine reconnection, emergence and cancellation (the adoption of an unsigned-flux convention means that $S_n > 0$ relates to emergence, while $S_n < 0$ relates to cancellation). Hence

$$\Delta\psi_n = R_n + S_n. \tag{10}$$

This decomposition, however, is not unique, as can easily be seen by the fact that

$$\Delta\Phi_a = \sum_{n=1}^{N_d} M_{an} S_n, \tag{11}$$

which is consistent with no reconnection ($R_n = 0$). Thus, in order to quantify the reconnection R_n occurring in a field in which $\Delta\Phi_a$ and $\Delta\psi_n$ are measured, additional information that allows the determination of S_n must first be introduced.

In the following section, the scenario in which emergence and cancellation of flux are prohibited is considered, so that only the time taken to recycle coronal flux due to fragment motions is measured. Section 5 then deals with the effects of emergence and cancellation on the recycling time of coronal flux due to reconnection.

4. Scenario 1: Excluding Emergence and Cancellation

Initially, fields with $\Delta\Phi_a = 0$ are considered. By Equation (11), this means that $S_n = 0$ for all n. This is achieved in the following way: if a fragment a is identified, which exists in both the initial and final frames, then the flux of a is adjusted in both frames so that it is equal to the mean of its values in frame i and frame f. However, since the four processes of emergence, fragmentation, coalescence and cancellation occur, this must also be taken into account when adjusting the fluxes.

Generally, if fragments that are born or die between frames i and f are excluded, the fluxes in frame i are adjusted in one of the following two ways.

1. If the fragment a in frame i is not just about to coalesce, then its flux Φ_a^i is adjusted such that

$$\Phi_a^i \to \frac{\Phi_A^f + \Phi_a^i}{2},$$

where Φ_A^f is its corresponding flux in the frame f. If the fragment a is not about to fragment, then $\Phi_A^f = \Phi_a^f$, the fragment's flux in frame f. If a is just about to fragment, then

$$\Phi_A^f = \sum_{j=1}^{p} \Phi_{a_j}^f,$$

where $\Phi_{a_j}^f$ are the fluxes of the p fragments into which a fragments.

2. If m fragments in frame i are just about to coalesce, then the fluxes of each of the a_j fragments ($j = 1, \ldots, m$) are adjusted such that

$$\Phi_{a_j}^i \to \frac{\Phi_{a_j}^i}{\Phi_A^i}\left(\frac{\Phi_A^f + \Phi_A^i}{2}\right),$$

where Φ_A^f is as previously defined and

$$\Phi_A^i = \sum_{j=1}^{m} \Phi_{a_j}^i,$$

namely, the sum of the fluxes of the m fragments that are about to coalesce.

Similarly, if fragments that are born or die between frames i and f are again excluded, then the fragments in frame f must also have their fluxes adjusted in one of the following two ways.

1. If the fragment a in frame f has not just been involved in fragmentation, then its flux Φ_a^f is adjusted such that

$$\Phi_a^f \rightarrow \frac{\Phi_a^f + \Phi_A^i}{2},$$

where Φ_A^i is its corresponding flux in the frame i. If the fragment a does not consist of newly merged fragments, then $\Phi_A^i = \Phi_a^i$, the fragment's flux in frame i. If a is comprised of newly merged fragments, then

$$\Phi_A^i = \sum_{j=1}^{p} \Phi_{a_j}^i,$$

where the $\Phi_{a_j}^i$ are the fluxes of the p fragments that merged.

2. If the fragment a has just merged with m fragments, then the fluxes of each of the a_j fragments ($j = 1, \ldots, m$) is adjusted such that

$$\Phi_{a_j}^f \rightarrow \frac{\Phi_{a_j}^f}{\Phi_A^f}\left(\frac{\Phi_A^f + \Phi_A^i}{2}\right),$$

where Φ_A^i is defined as above and

$$\Phi_A^f = \sum_{j=1}^{m} \Phi_{a_j}^f,$$

namely, the sum of the fluxes of the fragments that just merged.

The results obtained by these measures are provided in the following subsection.

4.1. Coronal flux recycling time due to reconnection driven by footpoint motions alone

By prohibiting the emergence and cancellation of flux between magnetogram pairs, it is possible to measure the changes in domain fluxes resulting from the motions of the fragments alone.

Assuming that each domain is either a "donor" or a "recipient" of reconnected flux, then the total amount of reconnected flux is

$$\Delta R = \frac{1}{2}\sum_{n=1}^{N_\mathrm{d}} |R_n|. \tag{12}$$

In this scenario, $R_n \equiv \Delta\psi_n$, since $S_n = 0$ in all domains.

The fraction of flux reconnected over time Δt is given by

$$f_R = \frac{\Delta R}{F}, \tag{13}$$

where F, the total flux in the system, is given by

$$F \equiv \sum_{n=1}^{N_\mathrm{d}} \psi_n = \frac{1}{2}\sum_{a=1}^{N_\mathrm{s}} \Phi_a. \tag{14}$$

If $f_R \ll 1$, then all field lines will be re-mapped after a time

$$\tau_r \equiv \frac{\Delta t}{f_R} = \Delta t \frac{\sum_{a=1}^{N_\mathrm{s}} |\Phi_a|}{\sum_{n=1}^{N_\mathrm{d}} |R_n|}, \tag{15}$$

where Δt is the time lapse between successive magnetograms, which here is 15 min. In the first instance, where all fragments that have just been born or just died are removed, the total flux F in the system is 1.91×10^{21} Mx. It is found that an average $8.12\% \pm 0.14\%$ of this flux (around 1.55×10^{20} Mx) is recycled between each pair of magnetograms. Using Equation (15), this results in a recycling time of $\tau_r = 3.08$ h (ranging from 3.03 and 3.13 h) for coronal field lines by motions of their footpoints alone.

By copying fragments that have just been born or have just died into the frame in which they are not present, similar figures are obtained. With F naturally being slightly higher here at 1.93×10^{21} Mx, it is found that, on average, $7.88\% \pm 0.14\%$ of flux (around 1.52×10^{20} Mx) is re-mapped between each pair of magnetograms, resulting in a period of $\tau_r = 3.17$ h for all the coronal field lines to be recycled. This has a range of 3.12–3.23 h if errors are taken into account.

However, the constant emergence and cancellation of flux through the photosphere is likely to have an effect on the re-mapping time for coronal field lines. The next section therefore details how an estimate of the effects of emergence and cancellation may be obtained.

5. Scenario 2: Including Emergence and Cancellation

In this section, changes in the strengths of the fragments from one frame to the next are included. Therefore, a boxcar smoothing method is applied to the time sequence of each fragment in order to remove spurious fluctuations in the fragment strengths. The effects of such smoothing are described in Appendix A.

Any effort to take into account emergence and cancellation of flux requires prior knowledge of the changes in source fluxes. In general, the change in the flux of a fragment a from frame i to frame f will be given by

$$\Delta\Phi_a = \Phi_a^f - \Phi_a^i.$$

However, it is again necessary to approximate what happens when fragments split or merge. Thus, in such cases, the change in flux of a fragment a is approximated by

$$\Delta\Phi_a = \frac{\Phi_a^f}{\Phi_A^f}\left(\Phi_A^f - \Phi_A^i\right).$$

If a is involved in fragmentation, then Φ_A^f is the sum of the fluxes of all the fragments that were involved in the fragmentation. Otherwise, $\Phi_A^f = \Phi_a^f$. Similarly, if a consists of newly merged fragments, then Φ_A^i is the sum of the fluxes of all the fragments in frame i that have merged by frame f. Otherwise, $\Phi_A^i = \Phi_a^i$, the corresponding flux for a in frame i.

Since infinity is included as a balancing source, then it too will have a change in strength. Thus, as changes from one system of flux balance to another are considered, the difference in these two fields comprises equal amounts of positive and negative flux. Hence, it is now possible to start thinking about obtaining a decomposition of Equation (11).

A natural starting point for considering emergence and cancellation is to assume that the processes of emergence and cancellation must occur at the photosphere, resulting in $S_n = 0$ for any domain n which is purely coronal. Assuming intuitively that emergence and cancellation occur through a set of flux tubes crossing the photospheric surface, then each flux tube will correspond to a domain, with the set of flux tubes forming a subset $\mathcal{T}$ of all domains. Henceforth, this shall be referred to as *pair-wise emergence/cancellation*. In the most straightforward version of this scenario, no source may belong to more than one flux tube, meaning that each flux tube links a pair of sources that must increase or decrease in tandem. However, even if pair-wise emergence/cancellation were occurring in practice, one could not realistically expect that measured changes in source fluxes $\Delta\Phi_a$, with inherent noise and other errors, will be exactly equal in each pair of sources. Thus, in order to make the analysis robust and mathematically well-posed, enough domains must be included in the set $\mathcal{T}$ so that its graph forms a *tree*. A tree is a graph in which all the vertices (here sources) are connected by a number of edges (domains) that is one fewer than the number of vertices, here $N_\mathrm{s} - 1$. Consequently, there will be one and only one path connecting any pair of vertices, thus ruling out the possibility of circuits (a circuit is a closed path containing a route that starts and ends at the same vertex, passing through other vertices along the way).

However, a general set of photospheric domains will contain many circuits, meaning that there will be numerous tree subgraphs that span the entire set of

sources. Thus, further information must be supplied so that the choice of tree is unique and is related to emergence and cancellation. An obvious assumption is that emergence/cancellation occurs between the closest pairs of sources, leading to a *minimum spanning tree*. Of course, infinity has been included as a source, which doesn't have a position. However, this minor difficulty is overcome by writing $D_{a\infty}$, the distance between the source a positioned at $\mathbf{x}_a$ and infinity, as

$$D_{a\infty} = D_{\max} + \frac{1}{|\mathbf{x}_a - \mathbf{x}_0|}.$$

where $\mathbf{x}_0$ is the centroid of all the sources and $D_{\max}$ is the maximum distance between any pair of sources. Thus, sources located at the edge of the region are preferentially chosen as the sources through which infinity is included in the tree.

So, with knowledge of the distances between pairs of sources, the minimum spanning tree is obtained, with the distances between the connected pairs of sources subject to the minimization. The minimum spanning tree is obtained using Prim's algorithm (Prim, 1957).

The incidence matrix $M_{an}^{(\mathcal{T})}$ may now be introduced, defined such that

$$M_{an}^{(\mathcal{T})} = \begin{cases} M_{an}, & \mathcal{D}_n \in \mathcal{T} \\ 0, & \mathcal{D}_n \notin \mathcal{T} \end{cases}, \tag{16}$$

where $\mathcal{D}_n$ represents the domain n. This allows Equation (11) to be rewritten as

$$\sum_{n=1}^{N_{\mathrm{d}}} M_{an}^{(\mathcal{T})} S_n = \Delta\Phi_a, \tag{17}$$

under the assumption that $S_n = 0$ for $\mathcal{D}_n \notin \mathcal{T}$. Since $\mathcal{T}$ is a tree, the matrix $M_{an}^{\mathcal{T}}$ is of full rank and may be inverted, giving

$$S_n = \sum_{a=1}^{N_{\mathrm{s}}} \left[M^{(\mathcal{T})}\right]_{\mathrm{na}}^{-1} \Delta\Phi_a. \tag{18}$$

In practice, Equation (16) is solved by locating a "leaf" on the tree, which is a vertex, representing source y, say, connected to only one edge, representing domain $\mathcal{D}_x$, say. This gives the relationship $S_x = |\Delta\Phi_y|$, which is trivial to solve. The vertex corresponding to source y and the edge corresponding to domain $\mathcal{D}_x$ are then "removed" from the graph, and the flux of the source z at the other end of domain x is decremented, such that $\Delta\Phi_z \to \Delta\Phi_z - S_x$. Hence, row a and column n are removed from Equation (16). The new graph still has one fewer edges than vertices, and is therefore still a tree. The process is repeated, solving for the next leaf and so forth, until all the S_n have been found. The final equation will contain two sources coupled by a single domain, and as such will be mathematically over-specified. However, since the system is in over-all flux balance, both of the remaining fluxes will be equal, and the remaining S_n may be determined from either one.

If $\mathcal{T}$ were unconnected, then, since complete flux balance is far from guaranteed for each disconnected component, Equation (16) would be over-constrained and could not be solved in general. Therefore, after obtaining the tree $\mathcal{T}$, a quick check is performed to ensure that the graph $\mathcal{T}$ is connected, which, of course, it always is.

In pair-wise emergence, at least in optimal conditions, the $\Delta\Phi_a$ vector takes the form of equal pairs corresponding to the emerging flux tubes. It can be shown that in this scenario S_n is non-zero in only those domains linking the pairs being considered, independent of which domains supplemented the graph $\mathcal{T}$ in order to obtain a tree. In practice, the addition of errors to a set of pair-wise emergences/cancellations will be manifested in non-zero (but presumably small) fluxes in additional domains.

5.1. PHOTOSPHERIC RECYCLING TIMES

By considering the change in the source fluxes, an estimate for the recycling time of photospheric flux due to emergence and cancellation may be obtained. The amount of emergence in all the sources is given by

$$\Delta S_+ = \frac{1}{2}\sum_{a=1}^{N_s} |\Delta\Phi_a|\Theta(\Delta\Phi_a), \tag{19}$$

where the Heaviside function $\Theta(x)$ picks out only the cases where the flux is increasing as emergence. The factor of $1/2$ is present since emergence affects a positive and a negative pole equally. Conversely, the amount of cancellation is given by

$$\Delta S_- = \frac{1}{2}\sum_{a=1}^{N_s} |\Delta\Phi_a|\Theta(-\Delta\Phi_a). \tag{20}$$

In a statistical steady state, one may define an average quantity ΔS that accounts for either emergence or cancellation as

$$\Delta S \simeq \frac{1}{2}(\Delta S_+ + \Delta S_-) \equiv \frac{1}{4}\sum_{a=1}^{N_s} |\Delta\Phi_a|. \tag{21}$$

The fraction of flux that emerges, which by the assumption of a statistical steady state is equal to the amount that cancels, is

$$f_S \equiv \frac{\Delta S}{F}, \tag{22}$$

where F is the total flux in the system, as given by Equation (14). Provided that the system is indeed in a statistical steady state, then all photospheric flux will be "recycled" by emergence or cancellation after a time

$$\tau_p \equiv \frac{\Delta t}{f_S} = \Delta t \frac{\sum_{a=1}^{N_s} |\Phi_a|}{\frac{1}{2}\sum_{a=1}^{N_s} |\Delta\Phi_a|}. \tag{23}$$

By including all changes in source fluxes in the calculation (i.e. changes due to births of fragments, deaths of fragments and fluctuations in their fluxes throughout their lifetimes), around 3.07×10^{19} Mx (some 1.6%) of the 1.92×10^{21} Mx of the flux F in the system is recycled every 15 min. Subsequently, by deploying Equation (15), a photospheric flux recycling time of 15.66 h is obtained. This figure is in fairly good agreement with that of Hagenaar (2001) who obtained a slightly shorter recycling time of 14 h for photospheric flux. Important factors that account for the difference in these estimates include the size of the area being studied – the region studied here is significantly smaller than that studied by Hagenaar (2001), plus the data set used here is of a much higher resolution too. Also, the two methods of calculating the recycling time differ greatly, with Hagenaar (2001) generally being much stricter in what is accepted as an emergence. (Hagenaar, Schrijver, and Title (2003) revised the previous figure by Hagenaar (2001) of 14 h to 8–19 h, which is still in agreement with the estimate obtained here).

5.2. Coronal recycling time due to emergence and cancellation

An estimate for the time taken to recycle the coronal field due to emergence and cancellation may also be obtained by considering the domains with $S_n \neq 0$. The total amount of emergence/cancellation in all domains is given by

$$\Delta S'_{\pm} \equiv \sum_{r=1}^{N_{\rm d}} |S_n| \Theta(\pm S_n), \tag{24}$$

Again, the Heaviside function picks out cases where flux is increasing/decreasing as emergence/cancellation. Following the same reasoning for $\Delta S_{\pm}$, an average quantity to account for *either* emergence or cancellation is defined:

$$\Delta S' \equiv \frac{1}{2}(\Delta S'_{+} + \Delta S'_{-}) = \frac{1}{2} \sum_{n=1}^{N_{\rm d}} |S_n|. \tag{25}$$

Using $\Delta S'$ instead of ΔS provides a time for *coronal flux recycling* due to emergence and cancellation:

$$\tau_{\rm e/c} \equiv \Delta t \frac{F}{\Delta S'} = \Delta t \frac{\sum_{a=1}^{N_{\rm s}} |\Phi_a|}{\sum_{n=1}^{N_{\rm d}} |S_n|}. \tag{26}$$

The photospheric recycling time should be longer than the corresponding coronal recycling time for recycling due to emergence/cancellation. This can be seen by taking the absolute value of Equation (17) and applying the triangle inequality:

$$|\Delta \Phi_a| \leq \sum_{n=1}^{N_{\rm d}} M_{an}^{(\mathcal{T})} |S_n|. \tag{27}$$

The equality only holds in the case that no source is involved in both emergence and cancellation simultaneously (since in this case all terms $M_{an}^{(\mathcal{T})} S_n$ are of the

same sign for a given source a). Although this is automatically true in the pair-wise emergence scenario, when each source is part of only one emerging flux tube, in the more general case of a tree of emergence domains it is possible for one source to simultaneously connect to both emerging and canceling domains at the same time. Substituting the inequality in expression (21) yields

$$\Delta S \leq \frac{1}{4} \sum_{a=1}^{N_s} \left(\sum_{n=1}^{N_d} M_{an}^{(\mathcal{T})} \right) |S_n| = \Delta S'. \tag{28}$$

Here use has been made of the fact that $\sum_a M_{an} = 2$ for any incidence matrix, since each domain connects exactly two sources. This inequality leads immediately to $\tau_{e/c} \leq \tau_p$.

At this point, it is not possible to obtain a value of the coronal recycling time due to emergence and cancellation that includes effects of the births and deaths of fragments. Since a birth (death) can inject (remove) a relatively large amount of flux in one go (due to the low cadence of the sequence of magnetograms studied here), this would wreak havoc on the decomposition for S_n. Such a problem would not be so pronounced with a much higher cadence, since the births (deaths) of fragments would be more smoothly traced, and there wouldn't be such a large amount of flux simply appearing (disappearing) between frames. Nevertheless, by including only the fluctuations in fragment fluxes throughout their lifetimes, coronal recycling times of $\tau_{e/c} = 2.25$ h and $\tau_{e/c} = 2.29$ h are found (the first figure is obtained by copying newly born/just died fragments into the frame in which they are not present, the second figure is obtained by removing said fragments from both frames altogether). The corresponding photospheric times, calculated by prohibiting births and deaths of fragments, are $\tau_p = 20.84$ h and $\tau_p = 21.01$ h. Thus, the time taken to recycle all the coronal flux due to emergence and cancellation is much less than the time taken to recycle all photospheric flux. This, as shall be seen, has dramatic consequences for the time taken for all coronal field lines to be re-mapped by reconnection.

5.3. Coronal recycling time due to reconnection driven by emergence, cancellation and motions of fragments

Having obtained an estimate for the amount of flux in each domain that may be attributed to emergence and cancellation, it is now possible to consider reconnection.

Changes in domain fluxes related to reconnection are given by subtracting the flux due to emergence/cancellation from each domain:

$$R_n = \Delta\psi_n - \sum_{a=1}^{N_s} \left[M^{(\mathcal{T})} \right]_{na}^{-1} \Delta\Phi_a. \tag{29}$$

An estimate of the amount of the coronal flux that is involved in magnetic reconnection may be obtained from

$$\tau_r \equiv \Delta t \frac{F}{\Delta R}, \tag{30}$$

where ΔR is found by substituting the R_n found here into Equation (12). In doing so, it is found that $17.87\% \pm 0.21\%$ (around 3.45×10^{20} Mx) of the 1.93×10^{21} Mx of coronal flux is re-mapped every 15 min, giving a recycling time of 1.399 h (ranging from 1.382 and 1.416 h). These figures are obtained by copying newly born/just died fragments into the frame in which they are not present; when the newly born/just died fragments are removed from the frame in which they are present, it is found that $17.61\% \pm 0.21\%$ (around 3.36×10^{20} Mx) of the 1.91×10^{21} Mx of coronal flux is re-mapped every 15 min, giving a recycling time of 1.420 h (ranging from 1.403 and 1.437 h).

The calculation of the flux (S_n) that has emerged or canceled in a given domain n linking a pair of sources is often larger than the observed net change in flux ($\Delta\psi_n$) when $\Delta\psi_n > 0$, so that the reconnected flux (R_n) is of the opposite sign to S_n (similarly, for $\Delta\psi_n < 0$, it is sometimes found that $S_n < \Delta\psi_n$). This implies that the field, initially assumed potential, reacts to emergence and cancellation of flux between frames by rearranging itself through the process of reconnection to a new equilibrium field (which is assumed to be potential). This is reasonable, since it would be unlikely that coronal domains simply swell from injection of flux without reconnection occurring. Thus, the changing of photospheric flux continually drives reconnection in the corona, enabling the field to remain close to potential.

6. Energy Dissipation

In this section, energy dissipation by means of separator reconnection is considered.

Generally, a given domain will be encircled by a closed ring of separators (Lau and Finn, 1990; Longcope and Klapper, 2002). The flux ψ_n^i in such a domain n may be obtained by defining a closed curve $\mathcal{K}$ which, for a coronal domain, is just the engirdling ring of separators, whilst for a photospheric domain, $\mathcal{K}$ is the section of the engirdling curve that is situated in the region $z \geq 0$, running from the photospheric points P to Q, combined with a line segment in the $z = 0$ plane joining P to Q. Integrating the magnetic potential $\mathbf{A}$ along $\mathcal{K}$ gives

$$\psi_n^i = \oint_{\mathcal{K}} \mathbf{A} \cdot \mathrm{d}\mathbf{l}, \tag{31}$$

where the direction of the integration proceeds parallel to the magnetic field along the separator.

Of course, there will also be isolated systems of flux where the field from a given source is completely enclosed by an unbroken fan surface from a single null – around

8.8% of nulls give rise to such domains in the region studied here. However, these domains account for only a small fraction of the total number of domains and, due to their nature, their fluxes will be altered primarily through emergence/cancellation of flux through the photospheric boundary. Thus, the consequences of the presence of these types of domain will not be considered here.

If the photospheric fragments are displaced so that the domain flux changes from ψ_n^i to ψ_n^f, then this will typically alter the net vacuum flux that $\mathcal{K}$ encloses by an amount $\Delta\psi_n$. However, Longcope (1996) points out that if the plasma is a perfect conductor, it will not permit any change in flux through $\mathcal{K}$. Therefore, a current ribbon with a total current I forms along the separator, with I flowing such that it generates a self-flux $\psi_n^{(cr)}(I)$ which cancels $\Delta\psi_n$. Hence

$$\psi_n^f + \psi_n^{(cr)}(I) = \psi_n^i + \Delta\psi_n + \psi_n^{(cr)}(I) = \psi_n^i. \tag{32}$$

Longcope and Cowley (1996) found that the quantities $\psi_n^{(cr)}(I)$ and I are related by

$$\psi_n^{(cr)}(I) = \mu_0 I \mathcal{L}, \tag{33}$$

where $\mathcal{L}$ is the differential inductance of the current ribbon. The precise expression for $\mathcal{L}$ can be quite complex, depending upon the current it carries; however, the purpose here is adequately served by approximating $\mathcal{L}$ by the length of the separator, L.

In order that non-potential energy may be stored in the corona, this requires that current densities are present without an accompanying electric field. Longcope (1996) proposed a scenario where the corona remains ideal for a period, during which currents gradually build up along each separator loop. When the build-up of current along a given loop exceeds a threshold value, it is assumed that some instability occurs, which permits an electric field $E_\parallel$ that in turn allows a change in flux through the loop $\mathcal{K}$, and reduces $\psi_n^{(cr)}$. Longcope (1996) also assumed that, when this process occurs, $\psi_n^{(cr)} \to 0$, so that all the energy above that of the potential energy is liberated and the field is returned to its vacuum state.

Here the aim is to obtain an estimate for the mean threshold current, I^*, at which the reconnection process is triggered. Time differentiating Equation (31) results in a version of Faraday's law

$$\frac{\mathrm{d}\psi_n}{\mathrm{d}t} = \oint_{\mathcal{K}} \frac{\partial \mathbf{A}}{\partial t}\,\mathrm{d}\mathbf{l} = -\int E_\parallel\,\mathrm{d}l = V_n, \tag{34}$$

where V_n is the voltage along the loop $\mathcal{K}$. Here the approximation

$$\frac{\Delta R_n}{\Delta t} \approx \frac{\mathrm{d}\psi_n}{\mathrm{d}t} \tag{35}$$

is made, where ΔR_n is the amount of reconnection associated with the domain n. Withbroe and Noyes (1977) obtained a heating rate of $H = 300\ \mathrm{W/m^2}$ for the quiet Sun. This may be related to this study by

$$H = \frac{I^* \langle V_n \rangle_{\mathrm{sep}}}{A} = \frac{I^*}{A} \left\langle \frac{\Delta R_n}{\Delta t} \right\rangle_{\mathrm{sep}} N_{\mathrm{sep}}, \tag{36}$$

where A is the area of the region, $\langle V_n \rangle_{\mathrm{sep}}$ is the mean voltage, I^* is the mean current along each separator, and N_{sep} is the number of separators in the region. Using the figures obtained by prohibiting emergence/cancellation, an I^* of 5.33×10^{10} A is obtained by removing all fragments that have just been born or died, and a similar figure of $I^* = 5.45 \times 10^{10}$ A is found by copying the newly born/just died fragments into the frame in which they are not present.

However, in the example where emergence and cancellation during the lifetimes of fragments are allowed, much lower values of I^* are found. By using ΔR in order to obtain $\langle V_n \rangle_{\mathrm{sep}}$, a value of 2.42×10^{10} A is found in the scenario whereby fragments that are newly born/just died are copied into the frame in which they are not present (by removing newly born/just died fragments from the frame in which they are present, a similar figure of 2.44×10^{10} A is found).

These values make sense when the difference in recycling times for the two representations (i.e. including and excluding emergence and cancellation) are considered. By disallowing emergence and cancellation, it is found that much less reconnection takes place. Thus one should naturally expect larger currents to build up. In the case when emergence and cancellation are allowed, however, the abundance of reconnection events means that the threshold current for allowing reconnection and the subsequent dissipation of energy must be lower for the given heating rate.

The figures above provide an indication as to the sort of values that should be expected from current-ribbon models of the quiet Sun, where currents are confined to magnetic separators.

Longcope (1998), in contrast, applied a current ribbon model to the flare of 7 January 1992, and suggested maximum currents of the order 10^{11} A were flowing along the associated separators. Here, the estimates for quiet-Sun separators suggest figures between 1 and 10 times smaller.

7. Conclusions

Examining changes in the connectivity of potential fields based on observed magnetograms has shown that there is quite a gulf in the recycling time of coronal flux compared with that for photospheric flux.

By identifying discrete fragments in a 12-h sequence of magnetograms, it is found that the time taken for all photospheric flux to be recycled is around 15.7 h. This is in fairly good agreement with the figures of 14 h obtained by Hagenaar (2001) and 8–19 h obtained by Hagenaar, Schrijver, and Title (2003), considering

the relatively small region and small time interval used here, and the completely different approaches to the calculations.

Whilst the recycling time for photospheric flux has been known for several years, until now there have been no estimates for the time taken to recycle the magnetic field in the corona. Such a calculation has been presented here. By considering a *pair-wise emergence/cancellation* scenario, whereby new flux emerges/cancels in flux tubes through a tree of domains linking pairs of closest photospheric flux sources, it is estimated how much of the change in domain fluxes is a consequence of emergence and cancellation of flux in the photosphere. In this way, it is found that emergence and cancellation of photospheric flux will recycle all coronal field lines in around 2.3 h.

The time taken to recycle the coronal field due to reconnection, which is of particular interest since reconnection is believed to be the primary means of heating the corona over the quiet Sun, has also been calculated here. By considering two scenarios, one in which the processes of emergence and cancellation are prohibited, and another in which the change in magnetic flux domains due to emergence and cancellation is estimated, it is found that the coronal flux is reconnected much more quickly in the presence of emergence and cancellation. If the motions of magnetic flux fragments were the only mechanism driving reconnection in the corona, it is surmised the process would take around 3 h to completely re-map all coronal field lines. However, by allowing emergence and cancellation as well, a much lower estimate of around 1.4 h is found.

This implies that the two main driving forces behind reconnection in the corona, namely reconnection driven by motions of fragments and reconnection driven by emergence and cancellation of flux, are comparable in their importance. The first estimate of 3 h indicates that even if emergence and reconnection were not occurring, the coronal magnetic field would still be entirely replaced in a relatively short time interval. The second estimate of 1.4 h implies that reconnection continually occurs in reaction to the emergence and cancellation of flux in the photosphere, which seems reasonable, as the coronal field is unlikely to allow domains to swell too much from injection of flux without responding in some way (similarly with reduction of flux due to cancellation). Hence, the changing of photospheric flux continually drives reconnection in the corona, enabling the field to remain close to potential.

All this will naturally have consequences for coronal heating. In this study, observed heating rates have been used, along with the findings presented here, to predict the consequences for energy dissipation due to separator reconnection. It is shown that the observed changes in domain fluxes will result in an average current density of around 5×10^{10} A for reconnection due to motions of flux fragments alone, whereas if reconnection due to emergence and cancellation is included, a lower average current density is produced of around 2×10^{10} A. This points to the fact that a higher rate of reconnection implies that the currents flowing along the separators during reconnection will generally be lower, as expected.

The model presented here does, however, have its limitations. Flux motions, caused by granular flows, which are unobservable in current magnetograms and occur within fragments (which have a finite geometrical extent), are neglected here. These would in turn cause more reconnection of field lines within domains, and would hence reduce the recycling time further. To some degree, however, the effects of neglecting such dynamics in the model are offset by the fact that potential fields are used to model the corona, since a potential field permits no stress and therefore reconnection occurs instantaneously. Work by Parnell and Galsgaard (2004), which examined reconnection between two driven flux patches initially separate and connected to an ambient coronal field, showed that in a potential field, the sources reconnect all their flux in a quarter of the time taken by a full MHD evolution.

The mean reconnection time for coronal flux presented here will nevertheless have a number of interesting applications in future. Indeed, the analysis may be extended to provide a distribution of energy release magnitudes for the solar corona, and it could also be adapted to show how reconnection in the quiet Sun may account for the background population of non-thermal electrons observed by RHESSI. Furthermore, the frequent reconnection episodes will most likely launch a spectrum of waves that are a necessary input to models of solar wind acceleration (e.g. Axford and McKenzie (2002)). Knowledge of the recycling rate of the coronal magnetic field may also be of relevance to studies of the anomalous diffusion of plasma through the corona and abundance variations.

Appendix: A. Effects of Data Smoothing

Preparing magnetogram data for the purpose of extrapolation requires the use of thresholds in order to separate genuine signals from the noise that is inherent in magnetic field observations. In the data studied here, where fragments are tracked not only spatially but also temporally, two levels of threshold are used so that fragments whose strengths fluctuate above and below the upper threshold are tracked properly and not simply recorded as a series of births and deaths.

Despite the use of two thresholds to minimize the counting in and out of pixels with values near the upper threshold level, the total flux in each of the fragments does of course include contributions from noise in the pixels. As the method outlined in Section 5 for calculating emergence and cancellation in the fragments counts all changes in the fluxes of the fragments between frames as being emergences or cancellations, this inevitably results in an over-estimation of the amount of emergence and cancellation that is occurring.

Thus, in order to reduce the effects outlined above, data smoothing is applied to the time sequence of each fragment's flux. The algorithm used for the smoothing is a boxcar smoothing algorithm. This essentially relies on an integer parameter w which defines the width of the "smoothing window" (i.e. the number of neighboring

data points used for the smoothing of a given data point). Varying the size of w subsequently varies the amount of smoothing that occurs, therefore varying the amount of emergence and cancellation that occurs.

Before proceeding any further, it is worth pointing out that since mergence and fragmentation may occur within the region of interest, it is not always possible to smooth over the entire lifetime of some fragments. In such cases, only the parts of the time sequence of the fragment's flux where no mergence or fragmentation occurs are smoothed. Of course, this will lead to peculiar jumps in the time sequences of such fragments across the points where mergence or fragmentation occur. In order to remove these anomalies, the fluxes of the fragments that are affected by mergence and fragmentation are adjusted in accordance with Section 4. In this way, it is assumed that fragments that either merge or split between a given pair of magnetograms witness no emergence or cancellation. This is an unavoidable consequence of using observed data in which mergence and fragmentation occur.

Ideally, a sensible amount of smoothing should be applied so that one may be certain that spurious fluctuations in the data due to noise in the magnetogram pixels are eradicated without compromising the profiles of the fragment fluxes too much. Whilst all recycling times given in the text are calculated using a smoothing window of width 7 frames (1.75 h), it is interesting to observe what happens to the recycling times when varying levels of smoothing are used. This is what is detailed here.

Figure 3 shows a couple of plots that demonstrate how the recycling time for photospheric flux, given by Equation (23), varies as the amount of smoothing deployed varies. Plot (a) shows the photospheric recycling time calculated by measuring all changes in the fluxes of the fragments, i.e. due to births of fragments, deaths of fragments and fluctuations in the strengths of fragments. From an initial recycling time of 10 h in the case where no smoothing is deployed, the graph asymptotes towards a figure of around 46 h. This would essentially be the time taken to recycle all photospheric flux were the strengths of each fragment constant over its lifetime. Plot (b) in Figure 3 shows the recycling times calculated when changes in flux associated with the births and deaths of fragments are ignored. In such a scenario, one would expect the recycling time to tend to infinity as the smoothing is increased, since the profiles of the fragments tend to one in which the fragment fluxes are constant over their lifetimes. This is clearly seen to be happening in the plots.

Corresponding coronal recycling times due to emergence and cancellation, given by Equation (26), are shown in Figure 4(a). Again, the effects of the births and deaths of fragments have been neglected in the calculation of these values, meaning that as the amount of smoothing increases, the recycling time tends towards infinity. Comparing plot (b) in Figure 3 with Figure 4(a) suggests that the photospheric recycling time tends to infinity much more quickly than the coronal recycling time. This is fairly intuitive behavior, since one would expect a given amount of recycling in the photosphere to result in substantially more recycling in the corona, where the flux is partitioned into complex domain structures that interconnect the multitude of sources.

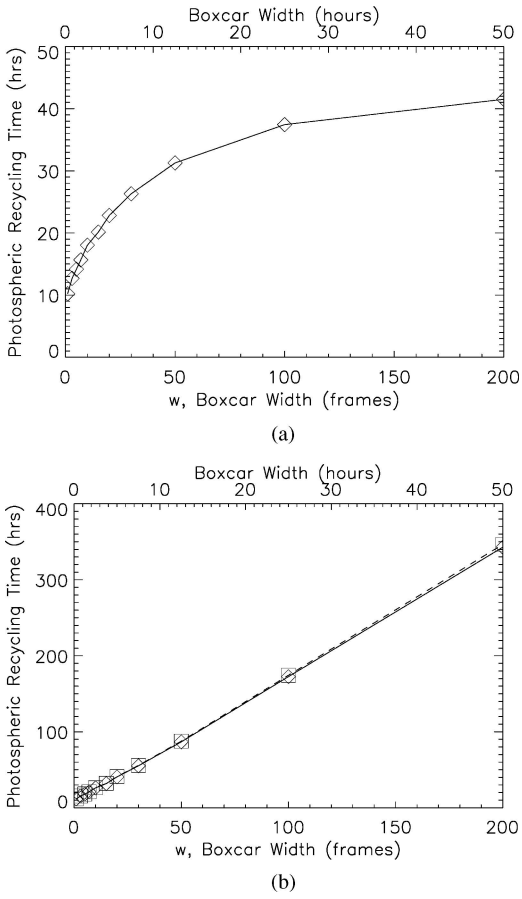

Figure 3. (a) Time taken (in hours) to recycle all photospheric flux versus boxcar width w used in the smoothing of the fluxes of the fragments. The diamonds indicate the values obtained for specific values of w. In this plot, births and deaths of fragments, along with the fluctuations in their fluxes, have been taken into account. (b) Time taken to recycle all photospheric flux when only fluctuations in the fluxes of fragments over their lifetimes are considered. The solid line and diamonds indicate values obtained when newly born/just died fragments are copied into the frame in which they are not present, whilst the dashed line and squares indicate values obtained when newly born/just died fragments are removed from the frame in which they are present.

The recycling times due to reconnection are displayed Figure 4(b). The times are calculated using ΔR in Equation (30). It can clearly be seen how varying the amount of emergence that is occurring affects the time taken to recycle all the coronal flux due to reconnection. When there is very little data smoothing applied, reconnection driven by emergence and cancellation of flux dominates over reconnection resulting from fragment motions, giving a recycling time of $\sim$0.78 h. However, as the amount of smoothing is increased, the flux recycling occurring as a result of emergence and cancellation becomes increasingly less significant. This relates to a scenario in

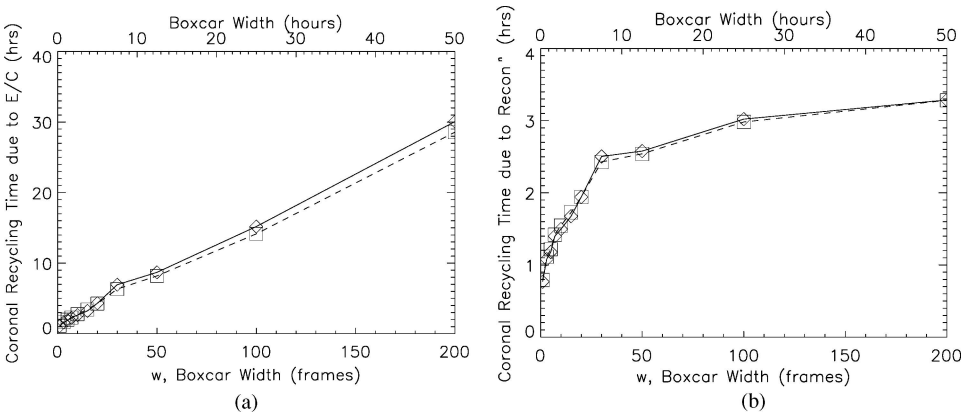

Figure 4. (a) Time taken (in hours) to recycle all coronal flux due to emergence and cancellation of flux in the photosphere versus boxcar width w used in the smoothing of the fluxes of the fragments. Again, the solid line and diamonds indicate values obtained when newly born/just died fragments are copied into the frame in which they are not present, whilst the dashed line and squares indicate values obtained when newly born/just died fragments are removed from the frame in which they are present. (b) Time taken to recycle all coronal flux due to reconnection versus boxcar width w used in the smoothing of the fluxes of the fragments.

which reconnection occurs only as a consequence of fragment motions. In the infinity limit, footpoint motions take just below 5 h to recycle all the flux.

Acknowledgment

The authors would like to thank the Particle Physics and Astronomy Research Council for financial support.

References

Axford, W. I. and McKenzie, J. F.: 2002, *Adv. Space Res.* **30**, 505.
Beveridge, C., Priest, E. R., and Brown, D. S.: 2002, *Solar Phys.* **209**, 333.
Brown, D. S. and Priest, E. R.: 1999, *Proc. R. Soc.* **455**, 3931.
Brown, D. S. and Priest, E. R.: 2001, *Astron. Astrophys.* **367**, 339.
Close, R. M., Parnell, C. E., Longcope, D. W., and Priest, E. R.: 2004, *Astrophys. J.* **612**, L81.
Close, R. M., Parnell, C. E., Mackay, D. H., and Priest, E. R.: 2003, *Solar Phys.* **212**, 251.
Durney, B. R., Young, D. S. D., and Roxburgh, I. W.: 1993, *Solar Phys.* **145**, 207.
Hagenaar, H. J.: 2001, *Astrophys. J.* **555**, 448.
Hagenaar, H. J., Schrijver, C. J., and Title, A. M.: 2003, *Astrophys. J.* **584**, 1107.
Hughes, D. W., Cattaneo, F., and Kim, E.: 1998, *Studia Geophysica et Geodaetica* **42**, 328.
Lau, Y. T. and Finn, J. M.: 1990, *Astrophys. J.* **350**, 672.
Levine, R. H.: 1974, *Astrophys. J.* **190**, 457.

Lin, H.: 1995, *Astrophys. J.* **446**, 421.
Longcope, D. W.: 1996, *Solar Phys.* **169**, 91.
Longcope, D. W.: 1998, *Astrophys. J.* **507**, 433.
Longcope, D. W.: 2001, *Phys. Plasmas* **8**, 5277.
Longcope, D. W. and Cowley, S. C.: 1996, *Phys. Plasmas* **3**, 2885.
Longcope, D. W. and Kankelborg, C. C.: 1999, *Astrophys. J.* **524**, 483.
Longcope, D. W. and Klapper, I.: 2002, *Astrophys. J.* **579**, 468.
McKenzie, J. F., Banaszkiewicz, M., and Axford, W. I.: 1995, *Astron. Astrophys.* **303**, L45.
Meneguzzi, M. and Pouquet, A.: 1989, *J. Fluid Mech.* **205**, 297.
Moffat, H. K.: 1978, *Magnetic Field Generation in Electrically Conducting Fluids*, Cambridge University Press, Cambridge.
Parker, E. N.: 1981, *Astrophys. J.* **244**, 644.
Parker, E. N.: 1983, *Astrophys. J.* **264**, 642.
Parker, E. N.: 1988, *Astrophys. J.* **330**, 474.
Parnell, C. E.: 2001, *Solar Phys.* **200**, 23.
Parnell, C. E.: In preparation.
Parnell, C. E. and Galsgaard, K.: 2004, *Astron. Astrophys.* **428**, 595.
Parnell, C. E. and Priest E. R.: 1994, in *Proceedings of the 3rd SOHO Workshop* **ESA SP-373**, 149.
Parnell, C. E. and Priest, E. R.: 1995, *Geophys. Astrophys. Fluid Dyn.* **80**, 255.
Petrovay, K. and Szakály, G.: 1993, *Astron. Astrophys.* **274**, 543.
Priest, E. R. and Forbes, T. G.: 2000, *Magnetic Reconnection: MHD Theory and Applications*, Cambridge University Press, Cambridge.
Priest, E. R., Heyvaerts, J. F., and Title, A. M.: 2002, *Astrophys. J.* **576**, 533.
Prim, R. C.: 1957, *Bell Syst. Tech. J.* **36**, 1389.
Schrijver, C. J., Title, A. M., Ballegooijen, A. A. V., Hagenaar, J. H., and Shine, R. A.: 1997, *Astrophys. J.* **487**, 424.
Schrijver, C. J., Title, A. M., Harvey, K. L., Sheeley, N. R., Wang, Y. M., van den Oord, G. H. J., Shine, R. A., Tarbell, T. D., and Hurlburt, N. E.: 1998, *Nature* **394**, 152.
Spruit, H. C., Title, A. M., and Ballegooijen, A. A. V.: 1997, *Solar Phys.* **110**, 115.
Tobias, S. M.: 2002, *Phil. Trans. R. Soc. Lond. A* **360**, 2741.
Withbroe, G. L. and Noyes, R. W.: 1977, *Annu. Rev. Astron. Astrophys.* **15**, 363.